

X-Ray Magnetic Circular Dichroism at the K edge of Mn_3GaC

Manabu Takahashi

Faculty of Engineering, Gunma University, Kiryu, Gunma 376-8515, Japan

Jun-ichi Igarashi

Synchrotron Radiation Research Center, Japan Atomic Energy Research Institute, Mikazuki, Sayo, Hyogo 679-5148, Japan

(Dated: November 14, 2018)

We theoretically investigate the origin of the x-ray magnetic circular dichroism (XMCD) spectra at the K edges of Mn and Ga in the ferromagnetic phase of Mn_3GaC on the basis of an ab initio calculation. Taking account of the spin-orbit interaction in the LDA scheme, we obtain the XMCD spectra in excellent agreement with the recent experiment. We have analyzed the origin of each structure, and thus elucidated the mechanism of inducing the orbital polarization in the p symmetric states. We also discuss a simple sum rule connecting the XMCD spectra with the orbital moment in the p symmetric states.

PACS numbers: 78.70.Dm, 71.20.Be, 75.50.Cc

I. INTRODUCTION

X-ray magnetic circular dichroism (XMCD) has attracted much interest as a useful tool to investigate magnetic states¹. The spectra directly reflect the magnetic order at the $L_{2,3}$ edges of transition-metal compounds and at the $M_{4,5}$ edges of rare-earth compounds, because by photoabsorption the core electron enters the $3d$ or $4f$ states which constitute the magnetic order. Sum rules have been found useful to evaluate the orbital magnetization^{2,3,4}. On the other hand, at earlier time, it was not clear where the XMCD spectra at the K edge of transition-metal compounds come from, because the $4p$ states the core electron enters by photoabsorption are not the states constituting the magnetic order^{5,6,7}. One of the present authors and Hirai have analyzed the XMCD at the K edge of ferromagnetic metals, Fe, Co, and Ni, and have found that the spectra come from the $4p$ orbital polarization induced by the mixing to the $3d$ states at neighboring sites^{8,9}. Subsequent experiments and calculations reached the similar conclusion for several transition-metal compounds.^{10,11,12,13,14,15,16,17}

The above mechanism is a consequence of an extended character of $4p$ states, and is closely related to the mechanism of the resonant x-ray scattering (RXS) at the K edges of transition metals in several compounds^{18,19}. The RXS intensity on superlattice spots was considered to be a direct reflection of the orbital order in LaMnO_3 ²⁰, but subsequent studies based on band structure calculations have revealed that the RXS intensity arises mainly from the lattice distortion which modulates the $4p$ states in the intermediate state of the second order process of the RXS^{21,22,23}. Recently, ab initio calculations of the RXS spectra have been carried out for YTiO_3 and YVO_3 , having clarified the important role of lattice distortion^{24,25}.

Despite such progress, the underlying mechanism of inducing $4p$ orbital polarizations is not fully understood. The XMCD experimental data recently obtained in the ferromagnetic phase of Mn_3GaC ^{26,27} seems suitable to make clear the mechanism, because considerable signals

have been found not only at the K edge of Mn but also at the K edge of Ga. In this paper, we analyze the XMCD spectra at the K edges in Mn_3GaC through an ab initio calculation. We use the Korringa-Kohn-Rostoker (KKR) method within the muffin-tin (MT) approximation³⁴ in the local density approximation (LDA) scheme, and take account of the spin-orbit interaction (SOI). We neglect the core-hole potential in the final state. We expect that the final-state interaction is unimportant except for the Fermi-edge singularity, because it is known from the study of the XMCD in Fe, Co, Ni, that the spectra are well reproduced without taking account of the final-state interaction^{6,7,8,9}. This may come from the fact that the $4p$ states have small amplitude inside the MT sphere and thus are little subject to the core hole potential.

In Sec. II, we calculate the electronic structure in a ferromagnetic phase of Mn_3GaC . In Sec. III, we present the formulas for the XMCD spectra and derive a sum rule. We also discuss the calculated spectra in comparison with the experiment. Section IV is devoted to concluding remarks.

II. ELECTRONIC STRUCTURE

This material takes an “inverse” perovskite structure²⁸, as schematically shown in Fig. 1. It has an interesting magnetic property; the antiferromagnetic phase in low temperatures turns into a ferromagnetic phase in high temperatures through a first-order transition at 168 K²⁶. We carry out the band calculation assuming a ferromagnetic phase with the magnetization fixed to the opposite of the $[111]$ direction, although an antiferromagnetic phase may be stabler than the ferromagnetic phase. By fixing the magnetization direction, we neglect the small magnetic anisotropy. We define the density of states (DOS) inside the MT sphere at a Mn site and at a Ga site. On Mn sites, the DOS projected onto the d symmetric states is dominating near the Fermi level. The s and p symmetric

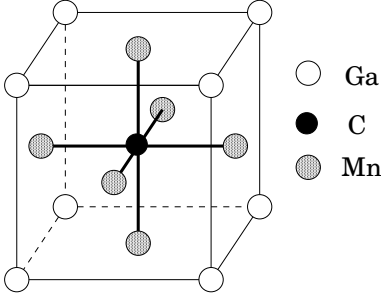


FIG. 1: Inverse perovskite-type crystal structure.

DOS's are found extremely small. The spin and orbital angular momenta, denoted as S and L in units of \hbar , are defined also inside the MT sphere. We get $S = 0.73$ and $L = 0.042$ in the d symmetric states, both of which are pointing to the $[111]$ direction, while we get $S = -0.0006$, $L = 0.00006$ in the p symmetric states (the $-$ sign means that the angular momentum is pointing to the opposite of the $[111]$ direction). The total magnetic moment becomes $-(2S + L)\mu_B = -1.50\mu_B$ per Mn. This value is consistent with the magnetization measurement²⁸ and the previous band calculations without taking account of the SOI^{29,30}. On the other hand, on Ga sites, the $3d$ states are located about 12 eV below the Fermi level. The s and p symmetric DOS's are found small above the Fermi level. Small angular momenta are induced due to the influence of the magnetic moments at Mn sites. We get $S = -0.011$, $L = 0.00046$ in the p symmetric states, and much smaller values, $S = 0.0021$, $L = -0.00041$, in the d symmetric states.

III. XMCD SPECTRA

We calculate the absorption coefficient, neglecting the core hole potential. Assuming that photons are propagating along the $[111]$ direction, we have the expressions for the right-handed (+) and left-handed (−) circular polarizations,

$$\mu_{\pm}(\omega) \propto \sum_{n,\mathbf{k}} \left| \int r^2 dr \int d\Omega \phi_{n,\mathbf{k}}(\mathbf{r})^* r Y_{1,\pm 1}(\Omega) R_{1s}(r) \right|^2 \times \delta(\hbar\omega - \epsilon_{n,\mathbf{k}}) \theta(\epsilon_{n,\mathbf{k}} - \epsilon_F), \quad (3.1)$$

where the spherical harmonic function $Y_{1,\pm 1}(\Omega)$ is defined with the quantization axis along the $[111]$ direction. The step function $\theta(x)$ ensures that the sum is taken over states above the Fermi level. The R_{1s} represents the $1s$ wave function of Mn or Ga, and $\phi_{n,\mathbf{k}}$ represents the wave function with the band index n , wave-vector \mathbf{k} and energy $\epsilon_{n,\mathbf{k}}$. In the actual calculation, we replace $\delta(\hbar\omega - \epsilon_{n,\mathbf{k}})$ by a Lorentzian form $(\Gamma/\pi)/((\hbar\omega - \epsilon_{n,\mathbf{k}})^2 + \Gamma^2)$ with $\Gamma = 1$ eV, in order to take account of the $1s$ core hole life-time width. The total absorption coefficient and the XMCD

spectra are defined by

$$\mu_0(\omega) = [\mu_+(\omega) + \mu_-(\omega)]/2, \quad (3.2)$$

$$\mu_c(\omega) = [\mu_+(\omega) - \mu_-(\omega)]. \quad (3.3)$$

The XMCD intensity arises from the p orbital polarization in the unoccupied states, as is obvious from Eq.(3.3). This quantity can be connected with the orbital moment in the p symmetric states as follows. Let the wave function be expanded in the MT sphere as

$$\phi_{n,\mathbf{k}}(\mathbf{r}) = \sum_{\ell,m,\sigma} f_{\ell,m,\sigma}^{n,\mathbf{k}} \psi_{\ell,m,\sigma}^{n,\mathbf{k}}(\mathbf{r}), \quad (3.4)$$

where $\psi_{\ell,m,\sigma}^{n,\mathbf{k}}(\mathbf{r})$ represents the wave function projected onto the state with the angular momentum $\{\ell, m\}$, and spin σ , and normalized inside the MT sphere. Then the orbital angular momentum in the p symmetric state is expressed as

$$L_p = \sum_{n,\mathbf{k},\sigma} (|f_{1,1,\sigma}^{n,\mathbf{k}}|^2 - |f_{1,-1,\sigma}^{n,\mathbf{k}}|^2) \theta(\epsilon_F - \epsilon_{n,\mathbf{k}}), \quad (3.5)$$

where the sum is taken over the occupied states. Note that, if the sum is taken over all the states both occupied and unoccupied, one may get $\sum_{n,\mathbf{k},\sigma} (|f_{1,1,\sigma}^{n,\mathbf{k}}|^2 - |f_{1,-1,\sigma}^{n,\mathbf{k}}|^2) = 0$. On the other hand, the absorption coefficient may be rewritten as

$$\mu_{\pm}(\omega) \propto \sum_{n,\mathbf{k},\sigma} \delta(\hbar\omega - \epsilon_{n,\mathbf{k}}) \theta(\epsilon_{n,\mathbf{k}} - \epsilon_F) |f_{1,\pm 1,\sigma}^{n,\mathbf{k}}|^2 \times \left| \int r^2 dr \int d\Omega \psi_{1,\pm 1,\sigma}^{n,\mathbf{k}}(\mathbf{r})^* r Y_{1,\pm 1}(\Omega) R_{1s}(r) \right|^2. \quad (3.6)$$

The last factor represents the transition probability from the $1s$ state to the p symmetric states, which varies little with respect to the energy of the p symmetric states above the Fermi level up to ~ 20 eV (within $\sim 10\%$ variation). This is because the p symmetric states are well approximated by the atomic $4p$ wave function on the region close to the center of atoms. Replacing the last factor by the value at the Fermi energy (denoted as $|S_F|^2$) in Eq.(3.6), we obtain approximately the relation,

$$\int^{\omega_2} \mu_c(\omega) d\omega \propto -|S_F|^2 L_p. \quad (3.7)$$

We need to introduce some upper cutoff ω_2 , because the transition probability is replaced by a constant $|S_F|^2$. It may be set by $\hbar\omega_2 = \epsilon_F + 20$ eV. This sum rule is an extension of the relation previously derived on the basis of the tight-binding model for Fe, Co, Ni metals^{8,9}.

Now we discuss the calculated spectra at the Mn K edge. Figure 2(a) and (b) show the total absorption coefficient $\mu_0(\omega)$ and the XMCD spectra $\mu_c(\omega)$ in comparison with the experiment²⁶. The experimental data are for a powdered sample under a small magnetic field $H = 0.6$ T at 200 K. The sample is in the ferromagnetic phase

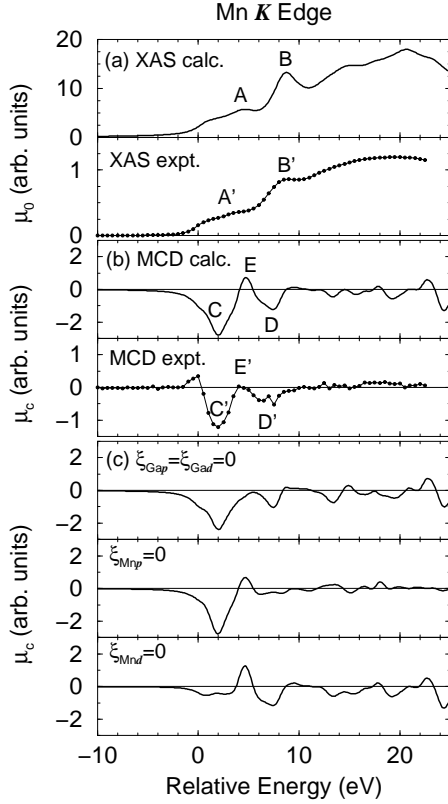


FIG. 2: (a) Total absorption coefficient $\mu_0(\omega)$, and (b) XMCD spectra $\mu_c(\omega)$ at the Mn K edge, as a function of photon energy. The origin of energy corresponds to the excitation to the Fermi level. The normalized intensities are magnified to 10^3 times. The experimental data are for a powdered sample in the ferromagnetic phase at $T = 200$ K²⁶. (c) XMCD spectra calculated with turning off the SOI on all the states at Ga sites, on the p symmetric states at Mn sites, and on the d symmetric states at Mn sites, respectively. $\xi_{Ab} = 0$ means that the SOI on the b symmetric states at A sites is turned off.

with the magnetization $\sim 0.8\mu_B$ per Mn, which value is smaller than the calculated one $1.5\mu_B$. The difference may be ascribed to a temperature effect, which usually reduces the magnetization. The calculated value of $\mu_c(\omega)$ is divided by the value of $\mu_0(\omega)$ at $\hbar\omega = \epsilon_F + 20$ eV, while the experimental XMCD spectra are divided by the value of the total absorption coefficient at the energy about 40 eV higher than the threshold. Both $\mu_0(\omega)$ and $\mu_c(\omega)$ are in good agreement with the experiment. For the total absorption coefficient, peaks A and B correspond well with shoulders A' and B' in the experimental curve. For the XMCD spectra, dips C, D, and peak E correspond well with the experimental ones C', D', and E'. Only one deviation from the experiment is that the small peak at the Fermi level is not reproduced. The intensity integrated up to ω_2 is found negative. This is consistent with the sum rule, Eq.(3.7), because the value of L_p is positive at Mn sites.

The XMCD spectra come from the orbital polarization in the p symmetric states, which may be induced by (i) the spin polarization in the p symmetric states through the SOI, and (ii) the orbital polarization at neighboring sites through hybridization. For making clear the inducing mechanism, we calculate the XMCD spectra at Mn sites with turning off the SOI on several specified states. The top panel among three panels of Fig. 2(c) shows the XMCD spectra with turning off the SOI on all the states at Ga sites. The spectra remain similar except for a slight suppression of peak E, indicating that the orbital polarization at Ga sites have little influence on the XMCD spectra at Mn sites. The middle panel in Fig. 2(c) shows the XMCD spectra with turning off the SOI only on the p symmetric states at Mn sites. Dip C keeps the similar shape, while dip D almost vanishes. This indicates that the p orbital polarization corresponding to dip D is induced by the spin polarization in the p symmetric states through the SOI. The bottom panel shows the XMCD spectra with turning off the SOI only on the d symmetric states at Mn sites. The intensity of dip C is drastically reduced, but dip D and peak E remains similar, indicating that the $3d$ orbital polarization gives rise to dip C. Within the MT approximation, the $3d$ orbital polarization cannot polarize the p orbital in the same Mn site, because the p - d Coulomb interaction is spherically averaged inside the MT sphere. Thus we conclude that the $3d$ orbital polarization at neighboring Mn sites induces the p orbital polarization corresponding to dip C through the p - d hybridization.

Next we discuss the XMCD at the Ga K edge. Figure 3(a) and (b) shows the calculated $\mu_0(\omega)$ and $\mu_c(\omega)$ in comparison with the experiment²⁷. Both $\mu_0(\omega)$ and $\mu_c(\omega)$ are in good agreement with the experiment. For the total absorption coefficient, peaks F and G correspond well with the experimental ones. Also, for the XMCD spectra, dip H, peak I and dip J correspond well with the experimental ones. The intensity integrated up to ω_2 is found negative. This is again consistent with the sum rule, because the value of L_p is positive at Ga sites.

For making clear the mechanism, we also calculate the XMCD spectra at Ga sites with turning off the SOI on several specified states. The top panel in Fig. 3(c) shows the XMCD spectra with turning off the SOI on the p symmetric states at Ga sites. Peak I and dip J are almost suppressed, indicating that the p orbital polarization corresponding to those structures is induced by the spin polarization in the p symmetric states through the SOI. On the other hand, dip H is half suppressed, indicating that the above mechanism works in a small part on dip H. The bottom panel shows the XMCD spectra with turning off the SOI on the d symmetric states at Mn sites. Dip J remains similar, dip H is half suppressed, and peak I is even enhanced. This indicates that the negative values are added to both dip H and peak I due to the coupling to the $3d$ orbital polarization at neighboring Mn sites.

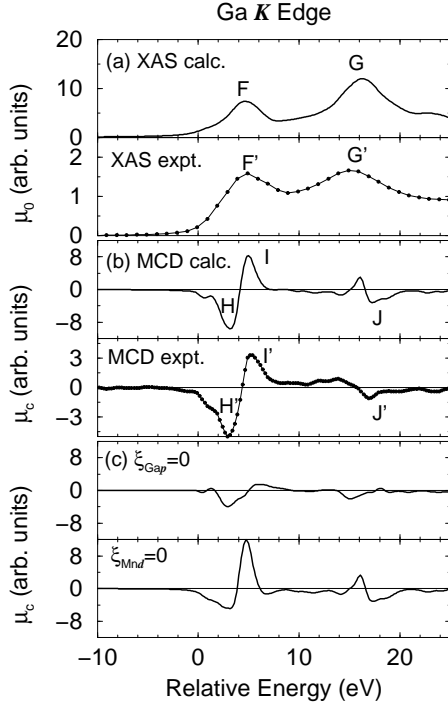


FIG. 3: (a) Total absorption coefficient $\mu_0(\omega)$, and (b) XMCD spectra $\mu_c(\omega)$ at the Ga K edge, as a function of photon energy. The origin of energy corresponds to the excitation to the Fermi level. The normalized intensities are magnified to 10^3 times. The experimental data are for a powdered sample in the ferromagnetic phase at $T = 200$ K²⁷. (c) XMCD spectra calculated with turning off the SOI on the p symmetric states at Ga sites, and on the d symmetric states at Mn sites, respectively. $\xi_{Ab} = 0$ means that the SOI on the b symmetric states at A sites is turned off.

As shown above, the calculation reproduces well the experimental curves. Only the exception is the small positive peak W at the Fermi level on Mn sites in the XMCD spectra (see Fig. 2). We might take it a small error, since the peak is small. However, in case of Mn_3ZnC , the similar positive peak at the Fermi level becomes large on Mn sites. To gain confidence in our calculation, we carry out a similar calculation for Mn_3ZnC , assuming a ferromagnetic phase. We get $S = 1.088$, $L = 0.019$ in the d symmetric states, and $S = -0.0003$, $L = -0.00005$ in the p symmetric states on Mn site. Figure 4 shows the calculated absorption and XMCD spectra at Mn K edge, in comparison with the experiment at $T = 300$ K (ferromagnetic phase). The positive peak at the Fermi level is clearly reproduced.

IV. CONCLUDING REMARKS

We have reported an ab initio calculation of the XMCD spectra at the K edges of Mn and Ga in the ferromagnetic phase of Mn_3GaC , by taking account of the SOI

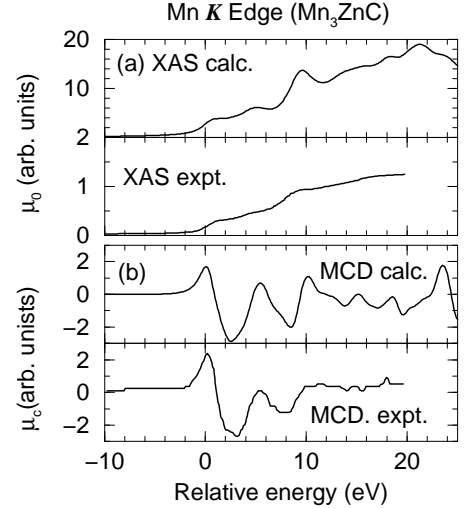


FIG. 4: (a) Total absorption coefficient $\mu_0(\omega)$, and (b) XMCD spectra $\mu_c(\omega)$ at the Mn K edge in Mn_3ZnC , as a function of photon energy. The origin of energy corresponds to the excitation to the Fermi level. The normalized intensities are magnified to 10^3 times. The experimental data are for a powdered sample in the ferromagnetic phase at $T = 300$ K²⁷.

in the LDA scheme. The calculated spectra show excellent agreement with the recent experiment. The spectra have explicitly been shown to arise from the p orbital polarization, and the mechanism of its induction has been fully analyzed; the associated process is identified for each structure. The present result may serve as a guide to analyze the K edge XMCD spectra in other materials. Such usefulness has been demonstrated for the ferromagnetic Ni metal. We have also derived a simple sum rule, which connects the XMCD spectra with the orbital moment, and have confirmed it works. Judging from the agreement of the calculated spectra with the experiment, we think that the effect of the 1s-core-hole potential in the final state is negligibly small.

The present finding is rather general and can be applied to other systems. To demonstrate this, we compare the XMCD spectra in Mn_3GaC with those in the ferromagnetic Ni metal. Figure 5 shows the latter quantity calculated with the same method as above. We divide $\mu_c(\omega)$ by $\mu_0(\omega_2)$ at $\hbar\omega_2 = \epsilon_F + 20$ eV. A large dip K appears above the Fermi level; it is half suppressed if the SOI is turned off either in the p symmetric states or in the 3d states. This behavior is similar to dip C in Mn_3GaC , although the contribution of the SOI in the p symmetric states is a little larger in Ni. On the other hand, a tiny dip L at high energy disappears without the SOI in the p symmetric states, similar to dip D in Mn_3GaC .

Finally we point out that this type of ab initio calculation can be applied to analyzing the magnetic RXS spectra at the K edge in transition-metal compounds^{31,32}, and may clarify the p orbital polarization in *antiferromagnetic* phases. According to our recent calculation of

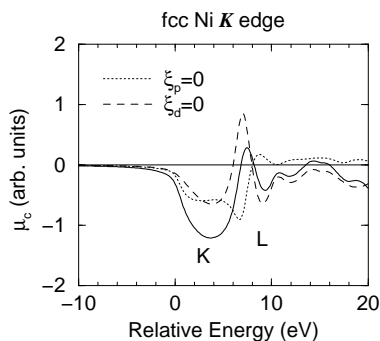


FIG. 5: Calculated XMCD spectra at the K edge in the ferromagnetic Ni metal, as a function of photon energy, which are divided by the total absorption coefficient at $\hbar\omega = \epsilon_F + 20$ eV and magnified to 10^3 times. The broken and dotted lines are values calculated with turning off the SOI on the p symmetric states and on the $3d$ states, respectively.

the magnetic RXS spectra in NiO^{33} , the main peak intensity almost disappears when the SOI on the $4p$ band is turned off. This finding is consistent with the above analysis, because the $4p$ states are located at ~ 10 eV higher than the Fermi level.

Acknowledgments

We would like to thank N. Kawamura and H. Maruyama for providing us the MCD experimental data prior to publication and for valuable discussion. This work was partially supported by a Grant-in-Aid for Scientific Research from the Ministry of Education, Science, Sports and Culture, Japan.

- ¹ G. Schütz and R. Wienke, *Hyperfine Interaction* **50**, 457 (1989).
- ² C. T. Chen, F. Sett, and S. Modesti, *Phys. Rev. B* **41**, 9766 (1990).
- ³ B. T. Thole, P. C. F. Sette, and G. van der Laan, *Phys. Rev. Lett.* **68**, 1943 (1992).
- ⁴ P. Carra, B. T. Thole, M. Altarelli, and X. Wang, *Phys. Rev. Lett.* **70**, 694 (1993).
- ⁵ G. Schütz, W. Wagner, W. Wilhelm, P. Kienle, R. Zeller, R. Frahm, and G. Materlik, *Phys. Rev. Lett.* **58**, 737 (1987).
- ⁶ H. Ebert, P. Strange, and B. L. Gyorffy, *J. Appl. Phys.* **63**, 3655 (1988).
- ⁷ S. Stähler, G. Schütz, and H. Ebert, *Phys. Rev. B* **47**, 818 (1993).
- ⁸ J. Igarashi and K. Hirai, *Phys. Rev. B* **50**, 17820 (1994).
- ⁹ J. Igarashi and K. Hirai, *Phys. Rev. B* **53**, 6442 (1996).
- ¹⁰ G. Y. Guo, *Phys. Rev. B* **57**, 10295 (1998).
- ¹¹ A. L. Ankudinov and J. J. Rehr, *Phys. Rev. B* **56**, R1712 (1997).
- ¹² J. P. Rueff, R. M. Galéra, C. Giorgetti, E. Dartyge, C. Brouder, and M. Alouani, *Phys. Rev. B* **58**, 12271 (1998).
- ¹³ C. Brouder, M. Alouani, and K. H. Bennemann, *Phys. Rev. B* **54**, 7334 (1996).
- ¹⁴ I. Yamamoto, S. Nagamatsu, T. Nakamura, T. Fujikawa, and S. Nanao, *J. Electron Spectroscopy and Related Phenomena* **125**, 89 (2002).
- ¹⁵ J. Chaboy, H. Maruyama, L. M. García, J. Bartolomé, K. Kobayashi, H. Kawamura, A. Marcelli, and L. Bozukov, *Phys. Rev. B* **54**, R15637 (1996).
- ¹⁶ J. Chaboy, L. M. García, F. Bartolomé, A. Marcelli, G. Cibin, H. Maruyama, S. Pizzini, A. Rogalev, J. B. Goedkoop, and J. Goulon, *Phys. Rev. B* **57**, 8424 (1998).
- ¹⁷ J. Chaboy, L. M. García, F. Bartolomé, H. Maruyama, A. Marcelli, and L. Bozukov, *Phys. Rev. B* **57**, 13386 (1998).
- ¹⁸ Y. Murakami, J. P. Hill, D. Gibbs, M. Blume, I. Koyama, M. Tanaka, H. Kawata, T. Arima, Y. Tokura, K. Hirota, et al., *Phys. Rev. Lett.* **81**, 582 (1998).
- ¹⁹ M. Noguchi, A. Nakazawa, S. Oka, T. Arima, Y. Wakabayashi, H. Nakao, and Y. Murakami, *Phys. Rev. B* **62**, R9271 (2000).
- ²⁰ S. Ishihara and S. Maekawa, *Phys. Rev. Lett.* **80**, 3799 (1998).
- ²¹ I. S. Elfimov, V. I. Anisimov, and G. Sawatzky, *Phys. Rev. Lett.* **82**, 4264 (1999).
- ²² M. Benfatto, Y. Joly, and C. R. Natoli, *Phys. Rev. Lett.* **83**, 636 (1999).
- ²³ M. Takahashi, J. Igarashi, and P. Fulde, *J. Phys. Soc. Jpn.* **68**, 2530 (1999).
- ²⁴ M. Takahashi and J. Igarashi, *Phys. Rev. B* **64**, 075110 (2001).
- ²⁵ M. Takahashi and J. Igarashi, *Phys. Rev. B* **65**, 205114 (2002).
- ²⁶ S. Uemoto, H. Maruyama, N. Kawamura, S. Umemura, N. Kitamoto, H. Nakao, S. Hara, M. Suzuki, D. Fruchart, and H. Yamazaki, *J. Synchrotron Rad.* **8**, 449 (2001).
- ²⁷ N. Kawamura, S. Uemoto, H. Maruyama, and D. Fruchart, private communication.
- ²⁸ D. Fruchart and E. F. Bertaut, *J. Phys. Soc. Jpn.* **44**, 781 (1978).
- ²⁹ M. Shirai, Y. Ohta, N. Suzuki, and K. Motizuki, *Jpn. J. Appl. Phys. suppl.* **32-2**, 250 (1993).
- ³⁰ A. L. Ovanovskii, R. F. Sabiryanov, and A. N. Skazkin, *Phys. Solid State* **40**, 1516 (1998).
- ³¹ W. Neubeck, C. Vettier, F. de Bergevin, F. Yakhov, D. Mannix, O. Bengone, M. Alouani, and A. Barbier, *Phys. Rev. B* **63**, 134430 (2001).
- ³² J. Igarashi and M. Takahashi, *Phys. Rev. B* **63**, 184430 (2001).
- ³³ M. Usuda, M. Takahashi, and J. Igarashi, unpublished.
- ³⁴ We add an empty sphere between neighboring Ga sites in order to reduce the interstitial volume. The MT radii used in the calculation are 0.25 in units of lattice constant so that the MT spheres are touching with one another.